Hyperstaticity for Ergonomic Design of a Wrist Exoskeleton

Mohammad Esmaeili, Nathanael Jarrasse, Wayne Dailey, Etienne Burdet, Domenico Campolo

▶ **To cite this version:**

HAL Id: hal-02110775
https://hal.archives-ouvertes.fr/hal-02110775

Submitted on 25 Apr 2019

Hyperstaticity for Ergonomic Design of a Wrist Exoskeleton

Mohammad Esmaeili[*,†,‡], Nathanaël Jarrassé[†], Wayne Dailey[‡], Etienne Burdet[‡] and Domenico Campolo[*]

[*]School of Mechanical and Aerospace Engineering, Nanyang Technological University, Singapore 639798
Email: {moha0157, d.campolo}@ntu.edu.sg
[†]Institute of Intelligent Systems and Robotics, CNRS - UMR 7222, University Pierre et Marie Curie, Paris, France
Email: jarrasse@isir.upmc.fr
[‡]Department of Bioengineering, Imperial College of Science, Technology and Medicine, London SW7 2AZ, UK
Email:{w.dailey12, e.burdet}@imperial.ac.uk

Abstract—Increasing the level of transparency in rehabilitation devices has been one of the main goals in robot-aided neurorehabilitation for the past two decades. This issue is particularly important to robotic structures that mimic the human counterpart's morphology and attach directly to the limb. Problems arise for complex joints such as the human wrist, which cannot be accurately matched with a traditional mechanical joint. In such cases, mechanical differences between human and robotic joint cause hyperstaticity (i.e. overconstraint) which, coupled with kinematic misalignments, leads to uncontrolled force/torque at the joint. This paper focuses on the prono-supination (PS) degree of freedom of the forearm. The overall force and torque in the wrist PS rotation is quantified by means of a wrist robot. A practical solution to avoid hyperstaticity and reduce the level of undesired force/torque in the wrist is presented, which is shown to reduce 75% of the force and 68% of the torque.

I. INTRODUCTION

Rehabilitation robotics experienced a strong and sustained growth of applications in the past four decades. These systems have evolved from the four degrees of freedom powered orthosis developed by CASE Institute of Technology in the early 1960's, which is generally recognised as the first rehabilitative manipulator [1], to recent state-of-the-art robots such as Bi-Manu Track [2]. In recent studies focusing on *neurorehabilitation*, most researchers targeted special therapy to recover the sensorimotor function and improve movement coordination in patients with lesions of the central or peripheral nervous system, e.g. after stroke [3–6]. In order to provide efficient training enabling patients to reacquire motor capabilities, it is crucial that rehabilitation robots should neither alter natural movements of the patients nor suppress any motor capability [7]. Therefore, special attention should be paid to robot workspace, fixation points, and control strategies to avoid any extra (unnatural) force or movement during therapy. On the other hand, haptic interfaces used to investigate the sensorimotor function in humans should avoid any resistance or reduction of the degrees-of-freedom that can bias the results [8].

Recently, haptic interfaces, exoskeletons and robots have been developed to promote self-rehabilitation [9], arm and wrist rehabilitation [10, 11]. The prono-supination (PS) joint of the forearm has received considerable attention in these devices. This joint is complex and cannot be modeled well as a simple pivot joint[1]. This issue was not taken into account during the design of most of these devices and it was assumed that alignment between a robot pivot joint and the virtual PS axis results in a kinematic match between the joints. Even when the device and forearm joint are perfectly aligned in the rest position, the unique configuration of the PS joint causes a misalignment as soon as movement is initiated. Thus, closing the (human+robot) mechanical loop with a "different" and simplified robotic joint leads to over-constrained configuration, i.e. hyperstaticity. As a consequence, uncontrolled interaction forces would arise as soon as misalignment occurs.

In this paper, we observe the importance of accounting for over-constrained attachments when designing a robot for rehabilitation. In particular we examine how the fixation of the human to the device necessitates attention when analyzing kinematic compatibility as presented in [12]. We developed a simple PS interface to investigate this issue. We applied the methodology from [12] and performed simple experiments to evaluate the amount of uncontrolled and undesired force that can be applied on the human wrist by a hyperstatic robotic device. We assessed the level of overall force and torque due to hyperstaticity on a simple device. We then present a practical solution to reduce the uncontrolled force/torque. This simple approach may be applied to commercial robots for reducing the level of undesired force/torque during operation and in the design of highly backdrivable devices.

II. PRESENTATION OF THE WRIST ROBOT

The Wrist Robot shown in Fig. 1 is a 1 active DoF device used to collect the data required to validate the design of wrist interfaces. Its kinematics are composed of one pivot whose axis is intended to be coincident with that of prono-supination.
Control (for gravity compensation) and data recording are implemented in LabView 2011 (National Instruments), in a timed-loop structure with a high priority control loop at 1 kHz. This control frequency is sufficient because the bandwidth of human movements is limited to 2-3 Hz and only slow movements are performed with the device. Data (force and position) from the 6-DOF force sensor (Mini40-E Transducer from ATI Industrial Automation, Inc.) and encoder (HEDL

---

[1]The movement of this joint is produced through the rotation of radius bone about the ulna while the ulna is almost steady. Therefore, the PS rotation axis changes during the movement.
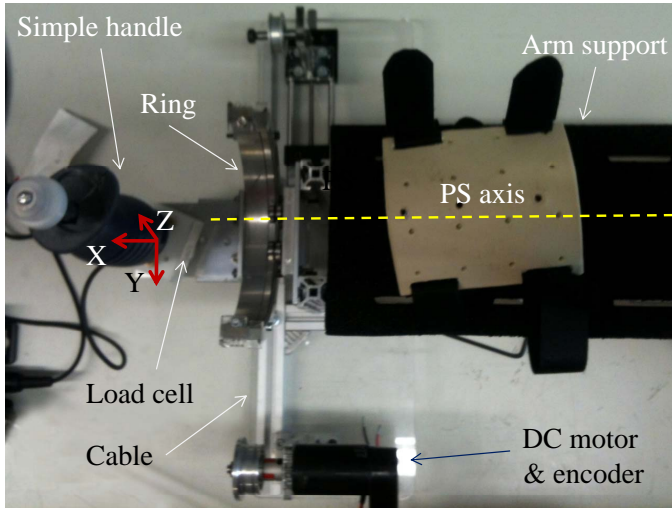
Fig. 1: **The initial wrist robot to study the reaction forces during prono-supination rotation.**

its two fixations (the human forearm is attached to the main body of the robot whereas the human hand is "attached" to
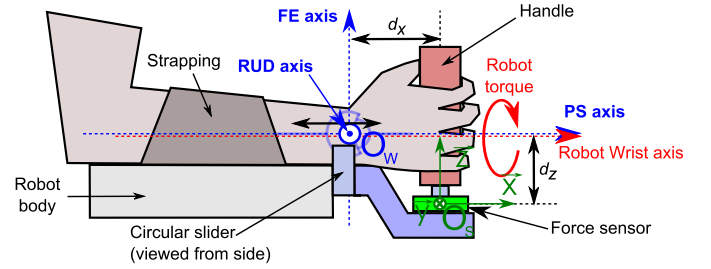

Fig. 2: **Human forearm attached to the Wrist Robot. Visualization of the force/torque sensor frame at O_s, the three rotation axes of human wrist (PS: Prono/Supination, FE: Flexion/Extension, RUD: Radiar/Ulnar Deviation) intersecting at the wrist joint center O_w, and that of the robot.**

5540 optical encoder, 3 channels, 500 lines per revolution, from Avago Technologies.) is sampled at the same frequency and is transferred to the main program, through a data acquisition card (PCI-6221, National Instruments), and used for gravity compensation. A DC motor (3242G012CR, stall torque: 181 *mNm*, from Faulhaber GmbH & Co.) was coupled to the ring via cables (reduction ratio: 3.9) to transmit the required driving torque. We used LSC 30/2 motor controller (from Maxon motor AG) to drive the DC motor.

III. METHODOLOGY

A. Hyperstaticity in the coupling

Exoskeletons are usually designed to replicate the kinematics of human limbs. However, it is impossible to precisely follow human kinematics with a robot. Human joint kinematics are very complex and do not correspond to conventional robot joints. Moreover, morphology drastically varies between subjects. Discrepancy, and thus kinematic incompatibility between the two structures seem unavoidable. If the connected bodies were rigid, the resulting hyperstaticity would lead to uncontrollable internal forces and immobilization.

In practice, rigidity is not infinite and mobility can be achieved thanks to the compliance of human tissues. A common principle to reduce hyperstaticity consists of adding passive DoFs at the fixation points between the robot and human. A method was recently introduced in [12], where a constructive technique was introduced to analyze the human-robot coupling, select the appropriate DoF to alleviate fixation, and design a mechanism guaranteeing global isostaticity and, consequently, a reduction in uncontrolled forces. Here the global methodology of [12] is applied to simplify the closed-loop mechanism consisting of the human wrist and the haptic prono-supination device and to select the best passive DoF for adding the mechanical loop.

B. Application

The schematic view of the Wrist Robot is depicted in the Fig. 2. The method from [12] was applied to this device and

the handle mounted on robot's end-effector), leading to the representation shown in Fig. 3. Considering that the robot
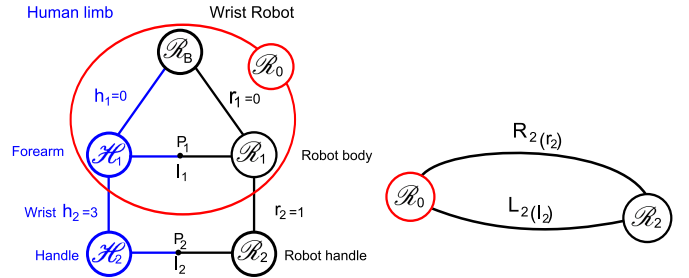

Fig. 3: **Schematic of the PS device and human forearm coupling**

segments and the human limbs are connected together through n fixations and that each fixation is a mechanism consisting of a passive kinematic chain, the total number of passive DoF to be added is given by the following set of equations:

$$\forall i \in 1 \cdots n, \sum_{j=1}^{i}(l_j + r_j) \geq 6i \tag{1a}$$

$$\forall i \in 1 \cdots n, \sum_{j=1}^{i-1}(l_j + r_j) + r_i \leq 6i \tag{1b}$$

$$\sum_{j=1}^{n}(l_j + r_j) = 6n \tag{1c}$$

where l_i is the connectivity of the fixation mechanism i (fixation can be an embedment - $l_i = 0$ - or can release several DoFs, such that: $\forall i \in \{1,..,n\}, \quad 0 \leq l_i \leq 5$), and r_i is the connectivity of each active robot joint. Considering that the human forearm is rigidly attached ($h_1 = 0$) to the robot body itself, which is fixed to the ground ($r_1 = 0$), we can simply consider the different bodies $\mathscr{R}_B, \mathscr{R}_1$ and $\mathscr{H}_1$ as a single rigid body $\mathscr{R}_0$. Thus, our goal is to define the number of DoF required to relieve the handle fixation level (i.e. l_2) and guarantee isostaticity (i.e. force controllability) even when the kinematics of the two chains (human and robot) differ.

Since only one fixation point is considered, only equation 1c must be applied on the Wrist Robot structure demonstrated in Fig. 3:

$$\sum_{j=2}^{n=2} l_j = 6 - r_1 = 1 \quad \Rightarrow l_2 = 5 \tag{2}$$

C. Selecting a solution

According to screw theory, the wrench describing the action of the robot r applied to the human limb h, at the wrist center O_w, expressed in the reference frame R_0 attached to the fixed body of the robotic interface, is:

$$\{\mathscr{W}_{O_w,\text{r}\to\text{h}}\} = \left\{ \begin{array}{c} \overrightarrow{F}_{\text{r}\to\text{h}} \\ \overrightarrow{\tau}_{O_w,\text{r}\to\text{h}} \end{array} \right\}_{R_0}, \ \overrightarrow{F}_{\text{r}\to\text{h}}, \overrightarrow{\tau}_{O_w,\text{r}\to\text{h}} \in \mathbb{R}^3$$

where $\overrightarrow{F}_{\text{r}\to\text{h}}$ are the forces applied on the human wrist by the robot, and $\overrightarrow{\tau}_{O_w,\text{r}\to\text{h}}$ are the torques applied at the wrist joint center O_w (see Fig. 2). Because force measurement is available at the sensor center O_s, we can derive the expression of $\mathscr{W}_{O_w,\text{r}\to\text{w}}$ from $\mathscr{W}_{O_s,\text{r}\to\text{h}}$. Therefore, by treating the mechanism and the wrist as a single rigid body:

$$\overrightarrow{\tau}_{O_w,\text{r}\to\text{h}} = \overrightarrow{\tau}_{O_s,\text{r}\to\text{h}} + \overrightarrow{O_w O_s} \wedge \overrightarrow{F}_{\text{r}\to\text{h}}$$

and thus:

$$\{\mathscr{W}_{O_w,\text{r}\to\text{h}}\} = \left\{ \begin{array}{cc} F_x & \tau_x^{O_s} - d_z F_y \\ F_y & \tau_y^{O_s} + d_x F_z^s + d_z F_x \\ F_z & \tau_z^{O_s} - d_x F_y \end{array} \right\} \tag{3}$$

where $(F_x, F_y, F_z, \tau_x^{O_s}, \tau_y^{O_s}, \tau_z^{O_s})$ are the force and torque components measured at the force/torque sensor center O_s and $\overrightarrow{O_w O_s} = [d_x \ d_y \ d_z]^T$. Using the wrench formulation, we can easily find alternative design solutions to "unlock" some DoFs at the wrist joint center through the addition of passive DoF mechanisms at other positions in the human-robot mechanical loop.

Based on the previous formulation of $\mathscr{W}_{O_w,\text{r}\to\text{h}}$ and the recommendations from [12] about how to select which Degrees of Freedom to release, we considered three aspects:
i) Velocities compatibility: we first examined the velocities of the relevant human limbs that are incompatible with the robot's kinematics. According to this analysis, all of the translational velocities along the PS, FE and RUD axis should be released, along with the two rotational velocities around the FE and RUD axes (see Fig. 4 below for axes definition).
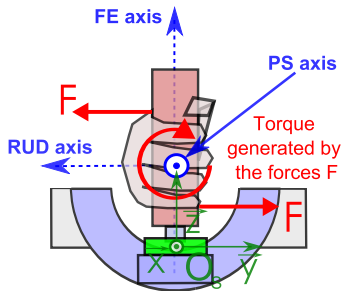

Fig. 4: **Generating torque around the PS axis through application of forces.**

ii) Force transmission: the wrist-robot is dedicated to the interaction with human prono-supination, thus only rotation around the PS axis should not be released in order to control the torque around this axis. Considering the coordination system in Fig. 2, the controlled torque would be $\tau_c = \|\tau_x\|$. The other generated forces and torques are uncontrolled and can be expressed as $F_{uc} = \sqrt{F_x^2 + F_y^2 + F_z^2}$ and $\tau_{uc} = \sqrt{\tau_y^2 + \tau_z^2}$.
iii) Consideration of human physiology: The moment around a main limb segment axis should not be transmitted directly (as this would deform the muscles), but rather be generated by the distant application of opposed forces. In this case, the solution was inherently included due to the handle as illustrated in Fig. 4.

Finally, the following DoFs were released in the design (see the orange arrows on Fig. 6): translation along the handle to prevent from force F_z application by the robot along the FE axis; translation along the forearm to prevent application of any force F_x along the PS axis; rotation around the FE axis to prevent the appearance of torque $\tau_z^{O_w}$ and the rotation around the RUD axis (to prevent from the projection of any torque $\tau_y^{O_w}$ generated by the robot or the human PS joint on the wrist flexion joint, and vice versa).

To simplify the design, this preliminary version of the robot does not incorporate translation release along the RUD axis at the handle as the fifth DoF, and thus does not avoid the building of force F_y. Redesigned fixation mechanisms lead to following wrench (considering also that $\overrightarrow{O_w O_s} = [0 \ 0 \ d_z]^T$):

$$\{\mathscr{W}_{O_w,\text{r}\to\text{h}}\} = \left\{ \begin{array}{cc} 0 & \tau_x^{O_s} - d_z F_y \\ 0 & 0 \\ 0 & 0 \end{array} \right\} \tag{4}$$

The improved version of the robotic PS interface, adding the new handle, called *Ergoexo*, can be seen in Fig. 5. As it is shown in Fig. 6, we mounted the *Ergoexo* on our wrist robot to conduct experiments.
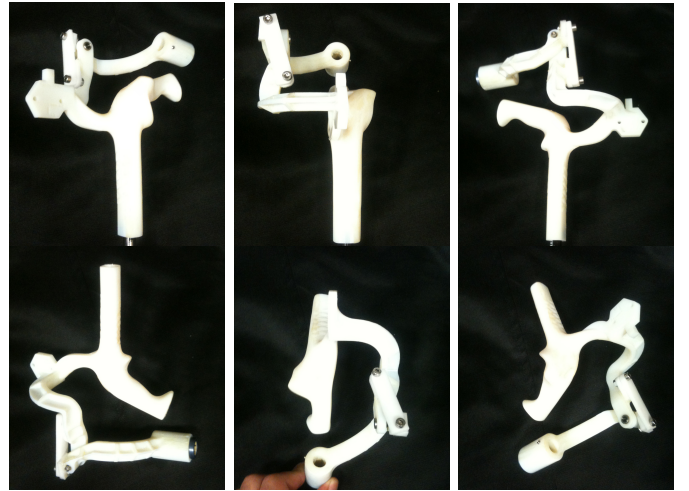

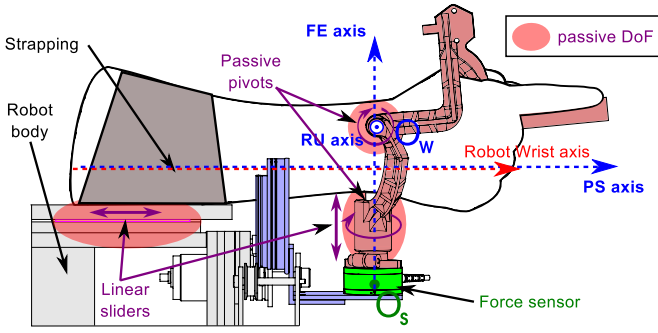Fig. 5: **Different views of the Ergonomic exoskeleton.**

Fig. 6: **Visualization of the force/torque sensor frame, the three rotation axes of human wrist, and the robot. Passive DoFs are represented by orange arrows.**

IV. EXPERIMENTS

A. Setup

Based on the presented solution the setup shown in Fig. 1 was modified to the Wrist Robot presented in Fig. 7 to validate the design. In order to study the effect of releasing passive DoF,
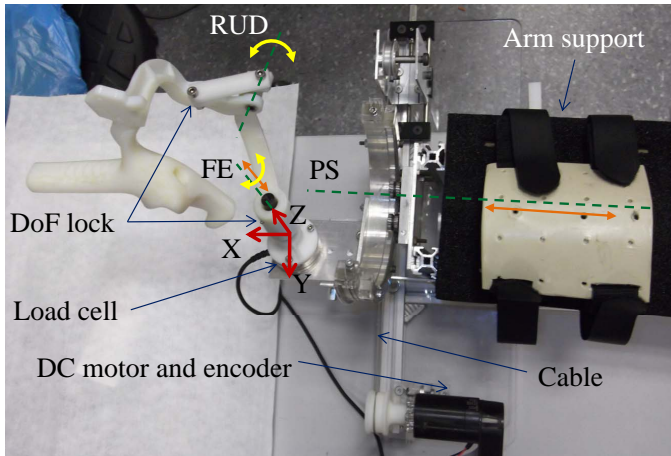

Fig. 7: **Improved Wrist Robot to study the reaction forces during prono-supination rotation.**

a set of parts were added to be able to block these passive DoF when needed. To ensure pure movement of wrist and minimal movement of elbow, shoulder, and torso during the experiment, the subject was asked to remain seated on a chair with his forearm strapped to the arm-support as illustrated in Fig. 1. The interaction force/torque was recorded with a (Mini40-E Transducer from ATI Industrial Automation, Inc.) load cell whose orientation and axes can be seen on Fig.6.

B. Protocol

Eight subjects, who declared to be right-handed, were asked to perform the following 'PS-rotation' movements. Using a mechanical linkage we initiated the same starting pose for all subjects. The subjects were instructed to grasp the handle firmly throughout the experiment, pronate their wrist to the limit of their range of motion, followed by supination to the opposite limit, and finally pronate back to the starting

point. We asked the subjects to rotate their wrist as far as they were comfortable without feeling pain. For each subject the force/torque was biased just before the first movement to cancel out the weight of the wrist. Experiment was conducted in three trials with the following conditions:
1. the passive DoFs were locked and gravity was not compensated,
2. the passive DoFs were locked but gravity was compensated,
3. the passive DoFs were released and gravity was compensated.

V. RESULTS AND DISCUSSION

In the following, the forces and torques shown are expressed at the wrist center O_w (see Fig. 6) as we are interested in reducing the uncontrolled effort at (human) joint level. As it is described previously, the only controlled component is $\tau_c = \| \tau_x \|$ and the rest are undesired and uncontrolled force/torque, i.e. $F_{uc} = \sqrt{F_x^2 + F_y^2 + F_z^2}$ and $\tau_{uc} = \sqrt{\tau_y^2 + \tau_z^2}$, which we aimed to reduce as much as possible.
To gain a general idea about the magnitude of force/torque in the presence and absence of extra passive DoFs, we calculated the mean of the total, controlled and uncontrolled force/torque over all subjects and all trials for each situation. Fig. 8 shows a significant reduction in the magnitude of the force/torque when gravity is compensated and even more when passive DoFs are freed.
Releasing the passive DoFs and gravity compensation reduce the total force from 3.1 N to 1.2 N (approximately %61.3 reduction) and total torque from 18.3 $N.cm$ to 7.9 $N.cm$ (approximately 56.7% reduction).
Fig. 9 illustrates the levels of the controlled torque and the uncontrolled force/torque versus the position averaged over all subjects. Fig. 8.c demonstrates that the method presented can reduce the amount of undesired force/torque by %70 and %67.9, respectively. This figure further shows that the gravity compensation is working correctly, as it is able to remove the part of the torque applied around the PS axis that is a function of the position, making the interaction torque uniform throughout the workspace. It can also be observed that releasing the passive DoF does not alter the force transmission of the Wrist robot (*i.e.* the controlled torque) as it does not affect τ_x. However, releasing the passive DoFs leads to an important beneficial reduction on the level of uncontrolled forces and torques.

Another interesting result shown in Fig. 9 is that gravity compensation eliminates dependency of the "controlled" force/torque on wrist position but also, surprisingly, it has the same effect on the "uncontrolled" directions. This could indicate a modification of the motor strategy change in the subjects due to gravity compensation activation. Alternatively, the torque generation around PS axis by the forearm muscles may produce additional small forces (or displacement leading to torque) in other directions. Hence, as soon as the amount of PS torque required to move the robot (τ_x) reduces, the forces on other directions are also reduced which is consistent with our observations in Fig. 9, that the amount of force/torque reduction due to gravity compensation is significant even on the axes that should not be affected by compensation.
Figure 10, allows more finely investigation on the effect of the releasing passive DoFs, by showing the effect of the
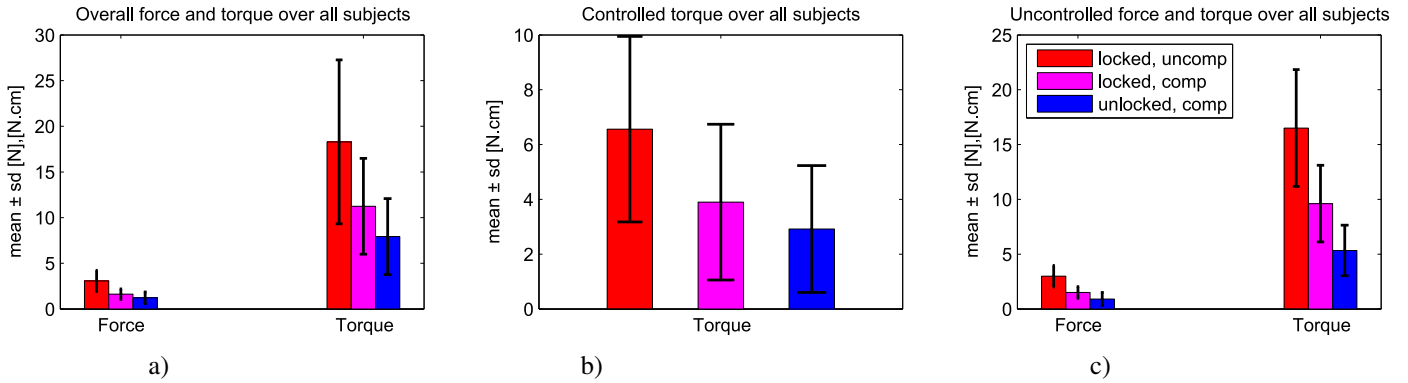
Fig. 8: **The amount of total (a), controlled (b) and uncontrolled (c) force and torque over all subjects, all trials.**
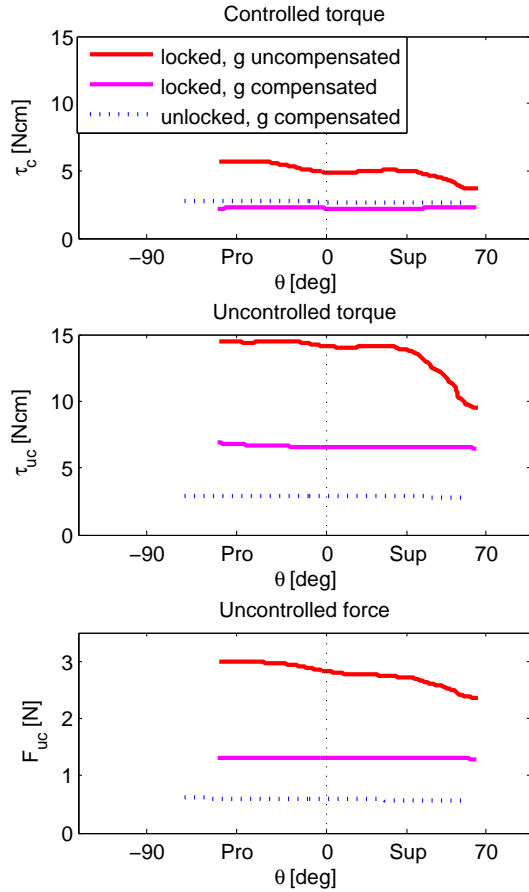

Fig. 9: **Controlled** $(\tau_c = \| \tau_x \|)$ **and uncontrolled** $(F_{uc} = \sqrt{F_x^2 + F_y^2 + F_z^2}, \tau_{uc} = \sqrt{\tau_y^2 + \tau_z^2})$ **force/torque for all subjects throughout the PS workspace.**

torque components τ_y and τ_z is observed, indicating a reduction of these uncontrolled torque components interacting with the RUD and FE degree-of-freedom of the subjects. Using the combined gravity compensation and passive DoF mechanism reduced τ_y from $13.3\,N.cm$ (maximum value) to $0.6\,N.cm$ and τ_z from $-6.0\,N.cm$ (maximum value) to $2.8\,N.cm$.

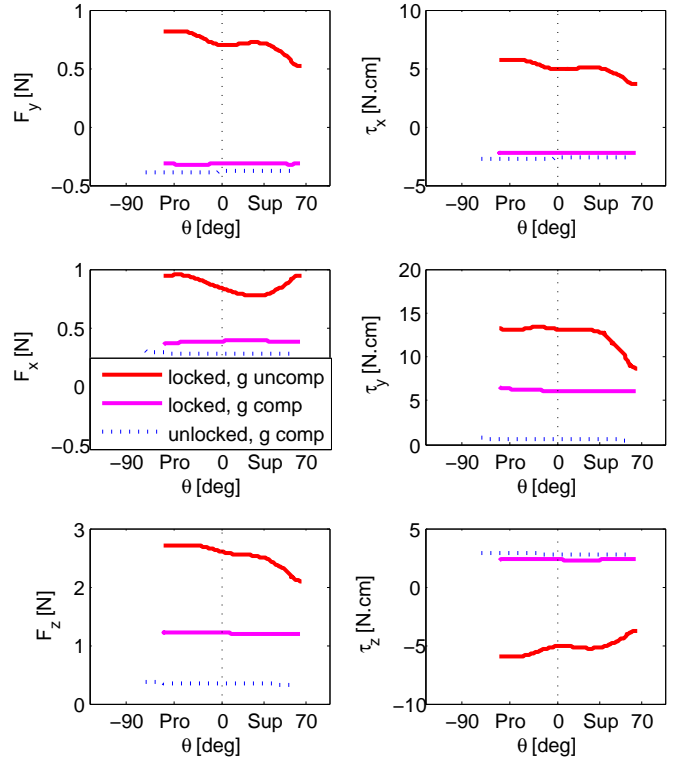As designing and manufacturing an ergonomic handle as the

Fig. 10: **The components of force/torque for all subjects throughout the PS workspace.** τ_x **is controlled and the rest are uncontrolled force/torque components.**

two tested conditions on every single component of force and torque. According to these results, releasing the passive DoFs seems not to significantly affect uncontrolled components, i.e. τ_z, F_x and even F_y, for which the force magnitude even increased slightly. However, comparing the levels of F_z for the locked-unlocked condition in Fig. 10 left side-bottom, reveals a massive reduction on this undesired force acting along side the handle. Similarly, an important decrease of the

Ergoexo could be time consuming and costly, and some finger strength might be needed to keep the handle in the proper position, using the perfect handles such as Ergoexo might not seem a convenient solution for other applications. Hence, along with the experiments with this handle, we evaluated the

performance of a simplified passive DoF handle. Taking the results of the Ergoexo into consideration, e.g. investigating Fig. 10, reveals that the translational and rotational DoFs about FE axis have a critical effect on uncontrolled force/torque. We thus simplified the handle to partly address the problem of hyperstaticity, by releasing only these two important DoFs. As it is shown in Table I, this simplified solution (i.e. introducing a sliding pivot joint in the handle) already allows to obtain 70% of the uncontrolled force/torque reduction capability of the Ergoexo handle.

TABLE I: **Mean and standard deviation of controlled and uncontrolled force and torque for Ergoexo and simplified handle. F_{uc}, τ_{uc} are uncontrolled force and torque, and τ_c is controlled torque.**

Movement condition		mean±SD of force/torque		
		F_{uc} (N)	τ_{uc} [N.cm]	τ_c [N.cm]
Ergoexo	locked, g uncomp	2.8±0.9	16.5±5.3	6.6±3.3
	locked, g comp	1.3±0.5	9.6±3.5	3.9±2.8
	unlocked, g comp	0.7±0.6	5.3±2.3	2.9±2.3
Handle	locked, g uncomp	3.1±0.1	16.7±0.5	5.5±1.4
	locked, g comp	1.8±0.3	6.3±3.0	3.8±0.4
	unlocked, g comp	0.9±0.1	6.2±1.7	2.2±1.8

VI. CONCLUSION

On account for gravity compensation we could decrease the magnitude of uncontrolled torques by approximately %42, see Fig. 8.c. Moreover, releasing passive DoFs, i.e. preventing hyperstaticity and its consecutive uncontrolled forces/torques, resulted in another approximately %45 reduction on the uncontrolled torques. Therefore, our results illustrates that accounting for passive DoFs could be as effective as considering gravity compensation in the reduction of undesired forces/torques for rehabilitation robots.

Another important result of this study is that the forces/torques seem to be linked, i.e. improving one force transmission results in improvement of other components. For instance, Fig. 10 shows that reducing the undesired τ_z yielded reduction of τ_x as well. Therefore it is useful to consider all forces in the design phase of the robot since a reduction of resistive force on one axis may modify the whole motor strategy.

Our results demonstrate how undesired forces might arise due to kinematic discrepancy between human and robot, and this discrepancy could instigate changes in motor strategy during robot therapy. Thus, the presented solution could be taken into account in the early phase of design of robots. It could also be applied to modify the fixation points of commercial robots in order to reduce the magnitude of reaction forces and avoid changes in motor strategy during the robotic therapy.

REFERENCES

[1] M. Hillman, "Rehabilitation Robotics from Past to Present A Historical Perspective," in *Advances in Rehabilitation Robotics*, Z. Bien and D. Stefanov, Eds. Springer Berlin Heidelberg, 2004, ch. 2, pp. 25–44.

[2] A. L. E. Q. van Delden, C. L. E. Peper, G. Kwakkel, and P. J. Beek, "A Systematic Review of Bilateral Upper Limb Training Devices for Poststroke Rehabilitation," *Stroke Research and Treatment*, vol. 2012, pp. 1–17, 2012.

[3] D. Mayhew, B. Bachrach, W. Z. Rymer, and R. F. Beer, "Development of the MACARM - a novel cable robot for upper limb neurorehabilitation." IEEE, Jul. 2005, pp. 299– 302.

[4] G. Rosati, P. Gallina, and S. Masiero, "Design, Implementation and Clinical Tests of a Wire-Based Robot for Neurorehabilitation," *IEEE Transactions on Neural Systems and Rehabilitation Engineering*, vol. 15, no. 4, pp. 560–569, Dec. 2007.

[5] H. I. Krebs, B. T. Volpe, D. Williams, J. Celestino, S. K. Charles, D. Lynch, and N. Hogan, "Robot-Aided Neurorehabilitation: A Robot for Wrist Rehabilitation," *Neural Systems and Rehabilitation Engineering, IEEE Transactions on*, vol. 15, no. 3, pp. 327–335, Sep. 2007.

[6] Y. Ren, S. Kang, H. Park, Y. Wu, and L. Zhang, "Developing a Multi-Joint Upper Limb Exoskeleton Robot for Diagnosis, Therapy and Outcome Evaluation in Neurorehabilitation," *IEEE Transactions on Neural Systems and Rehabilitation Engineering*, vol. PP, no. 99, pp. 1–10, 2012.

[7] N. Hogan and H. I. Krebs, "Interactive robots for neurorehabilitation," *Restorative Neurology and Neuroscience*, vol. 22, no. 3, pp. 349–358, Jan. 2004.

[8] D. Campolo, F. Widjaja, M. Esmaeili, and E. Burdet, "Pointing with the wrist: a postural model for Donders' law." *Experimental brain research*, vol. 212, no. 3, pp. 417–27, Jul. 2011.

[9] Z. Song and S. Guo, "Implementation of self-rehabilitation for upper limb based on a haptic device and an exoskeleton device," in *Mechatronics and Automation (ICMA), 2011 International Conference on*, Aug. 2011, pp. 1911 –1916.

[10] L. Lugo-Villeda, A. Frisoli, O. Sandoval-Gonzalez, M. Padilla, V. Parra-Vega, C. Avizzano, E. Ruffaldi, and M. Bergamasco, "Haptic guidance of Light-Exoskeleton for arm-rehabilitation tasks," in *Robot and Human Interactive Communication, RO-MAN 2009. The 18th IEEE International Symposium on*, Oct. 2009, pp. 903 –908.

[11] J. Oblak, I. Cikajlo, and Z. Matjacic, "Universal Haptic Drive: A Robot for Arm and Wrist Rehabilitation," *Neural Systems and Rehabilitation Engineering, IEEE Transactions on*, vol. 18, no. 3, pp. 293 –302, Jun. 2010.

[12] N. Jarrasse and G. Morel, "Connecting a Human Limb to an Exoskeleton," *IEEE Transactions on Robotics*, vol. 28, no. 3, pp. 697 –709, Jun. 2012.